EFFECT OF MICROSTRUCTURE ON THE EARLY STAGES OF CREEP DEFORMATION OF AN EXPERIMENTAL NICKEL BASE ALLOY

A. Ferrari

Laboratorio per la Tecnologia
dei Materiali Metallici non
Tradizionali - C.N.R.

P.O.Box 4394, Milano, (Italy)

ABSTRACT

The present study is dealing with an understanding of the factors controlling the creep behaviour, in the primary and second stage, of an experimental nickel base alloy similar to the wrought high-chromium alloy IN-597, intended for use as blades and other stressed parts in gas turbine burners, but with a low carbon content to reduce carbide precipitation as much as possible. The results of the creep tests carried out in the temperature range of practical use for this alloy, such as 700-850°C, show that during primary creep deformation the strain data follow very well the Li equation derived for this stage and that the creep rate parameters, coefficient K_1 and minimum creep rate $\dot{\varepsilon}_m$, can be related to the gamma prime precipitate particle morphology, dislocation motion mechanisms and grain boundary structures.

Introduction

Nickel base superalloys have been successfully used in gas turbines for components exposed to long periods of service at high temperatures. In general these alloys offer good mechanical properties and improved resistance to corrosion and oxidation due to a high chromium content and to the precipitation on the matrix of carbides and Ni_3 (Ti, Al) gamma prime particles. In the design of land-based gas turbines, the early stages of creep deformation of the materials selected must be considered so that the effects of structure, heat treatments and microstructural features on the creep characteristics are very important factors to be controlled.

This study is dealing with an understanding of the factors controlling the creep behaviour, in the primary and stationary stage, of an experimental nickel base alloy similar to the wrought high-chromium alloy IN-597 ([1]), intended for use as blades and other stressed parts in gas turbine burners, but with a low carbon content to reduce carbide precipitation as much as possible. The titanium and aluminum concentrations have been varied to obtain five alloys with a wide range of gamma prime volume fraction.

The present results describe the creep behaviour of the stronger experimental alloy, that is with higher gamma prime volume fraction; and the creep characteristics in the temperature range of 700-850°C were correlated with the microstructural features including grain size, gamma prime morphology and dislocation motion mechanisms.

Experimental details

The material used in this investigation has been supplied by Henry Wiggin as cast ingots with a maximum diameter of 100 mm and successively extruded at the National Physical Laboratory to 16 mm diameter bars ([2]). The chemical composition of this alloy, similar to the commercial IN-597 except for the carbon content, was as follows (weight percent) ([13]):

C	Cr	Co	Mo	Ti	Al	Nb	Ni
0.006	24.25	19.2	1.44	2.93	1.49	1.08	balance

Specimens having a 50 mm gauge length and 7.5 mm gauge diameter were cut from the bars.

Temperatures of 1200°C, 1150°C and 1080°C were chosen for the solution treatments in order to have materials with a wide range in grain size. The heat treatment of 50^h at 900°C was chosen as standard ageing treatment of gamma prime precipitates for the alloy considered. Only for some creep tests ageing treatment of 15^h or 90^h at 900°C were also carried out.

Standard techniques of optical metallography were employed for the examination of the structures of the extruded bars and creep tests. The determination of the grain sizes has been made on samples, cut in longitudinal direction, by means of the Snyder Graff method, using the following solution stirred at room temperature:

4 gr $CuSo_4$ + 20 cc HCl (30%) + 20 cc H_2O (distilled)

The study of the microstructures was carried out by means of the transmission electron microscopy on thinned samples cut from

Table I - Tensile and creep data of the experimental alloy.

Temperature (°C)	Stress (MN/m^2)	Rupture time (h)	Elongation (%)	Grain size (mm)	ε_m (h^{-1})	K_1 (h^{-1})
			4^h 1150°C/AC + 50^h 900°C/AC			
700	853	tensile*	7.5	-	-	-
	587	235	10.5	0.24	$3.1\ 10^{-4}$	-
	490	1633	5.4	-	$1.7\ 10^{-5}$	$2.4\ 10^{-1}$
	490	285**	0.5	0.22	$1.3\ 10^{-5}$	-
	442	2652	2.6	-	$1.8\ 10^{-6}$	-
750	412	530	3.8	0.23	$3.9\ 10^{-5}$	$1.2\ 10^{-1}$
	353	1350	2.5	-	$6.4\ 10^{-6}$	$3.2\ 10^{-2}$
800	743	tensile*	8.0	-	-	-
	314	16**	0.7	0.19	$2.8\ 10^{-4}$	$9.6\ 10^{-1}$
	274	71**	0.7	0.19	$6.1\ 10^{-5}$	$4.1\ 10^{-1}$
	258	180	3.2	-	$2.9\ 10^{-5}$	$2.3\ 10^{-1}$
	236	170**	0.3	0.20	$9.0\ 10^{-6}$	$5.0\ 10^{-2}$
	206	573	0.5	0.19	$5.6\ 10^{-6}$	$6.9\ 10^{-2}$
	157	1563	0.5	0.23	$1.7\ 10^{-6}$	$1.6\ 10^{-2}$
850	206	173	1.0	0.23	$1.1\ 10^{-5}$	$1.7\ 10^{-1}$
	157	414	1.4	0.22	$2.8\ 10^{-6}$	$4.8\ 10^{-2}$
			4^h 1150°C/AC + 15^h 900°C/AC			
800	265	121**	0.5	-	$2.4\ 10^{-5}$	$1.7\ 10^{-1}$
	206	597	0.8	0.22	$3.2\ 10^{-6}$	$3.7\ 10^{-2}$
			4^h 1150°C/AC + 90^h 900°C/AC			
800	206	193**	0.2	0.27	$6.8\ 10^{-6}$	$1.3\ 10^{-1}$
			4^h 1200°C/AC + 50^h 900°C/AC			
800	206	547	1.5	0.33	$4.2\ 10^{-6}$	$3.9\ 10^{-2}$
	147	1401	0.2	0.37	$7.7\ 10^{-7}$	$8.5\ 10^{-3}$
			4^h 1080°C/AC + 50^h 900°C/AC			
800	216	58**	0.2	0.13	$2.2\ 10^{-5}$	$1.6\ 10^{-1}$
	206	331	0.9	-	$1.3\ 10^{-5}$	-
	157	605	1.1	0.11	$5.3\ 10^{-6}$	$6.3\ 10^{-2}$

* 0.2% yield strenght: 700°C - 637 MN/m^2
800°C - 632 MN/m^2

** Tests interrupted during the second creep stage.

the as-treated materials and tested specimens. Electropolishing was carried out using the Bollman-Dupres method with a mixture of 6 percent perchloric acid and 94 percent acetic acid at an applied voltage of 39 V and a current density of about 0.5 A/cm^2. Precipitated phases at the grain boundaries and the grains themselves thinned at approximately the same rate permit study of all the microstructural features of the alloy. The films were then studied in a Siemens Elmiskop 1A electron microscope operating at 100 kV and in a Jeol 200 B operating at 200 kV.

The creep tests were conducted in creep testing machines Denison mod. T48 and Satec mod. EE and the specimens were gripped in holders fitted to a universal joint-type assembly to promote uniaxial loading. The extensometer system detected specimen strain as small as 10^{-5}. Tensile and creep-rupture tests were carried out on the alloy at temperatures between 700 and 850°C under stresses ranging from 600 to 150 MN/m^2, to cause elongations in the early stages of creep deformation between 10 and 1000 hours. Some of the tests were interrupted during the second creep stage and successively cooled under load to preserve the structure at this stage for electron microscopy examinations.

A quantitative separation of γ' particles from γ solid solution has been developed for the determination of gamma prime volume fraction of the alloy using anodic dissolution of the sample matrix in an aqueous electrolyte containing 1% ammonium sulfate and 1% citric acid in distilled water ([3]). Disks, 1 mm thick, were cut from specimens solution treated 4^h 1150°C and aged 1000^h at 700°C, 250^h at 800°C and 66^h at 900°C respectively; consequently the measurements were carried out on samples, with a γ' particle diameter greater than 400 Å, to avoid a partial dissolution of the small particles.

The extracted γ' was probably accompanied by a minor amount of carbides but no corrections for this contamination have been made because of the very low carbon content of the alloy. Finally, a factor of 1.04 was used to convert weight fraction to volume fraction.

Results

The various heat treatments and microstructural changes that occurred during testing resulted in a wide range of microstructural features. In effect, considerable variations were observed in grain size and gamma prime particle diameter. The gamma prime growth has been observed at 900°C by means of transmission electron microscopy examinations. The data of the analysis are somewhat lower than those available from the commercial alloy ([1]).

Gamma prime volume fraction has been determined as a function of the ageing treatments in the temperature range 700-900°C. Experiments indicated that, starting from the low temperatures, a volume fraction of about 25.0 and 24.5% resulted at 700 and 800°C respectively. When increasing temperature up to 900°C, the volume decreased down to 20.3%, indicating that in the higher temperature range there is a remarkable reduction in the volume fraction. In effect, the gamma prime solution temperature is probably near the value of 1050°C ([2]).

The grain sizes of the heat treated material vary. The approximate sizes of the grains of the material solution treated 4^h at 1200°C and 4^h at 1080°C were 0.35 and 0.12 mm respectively. For the remainder of the heat treatments the grains were approximately

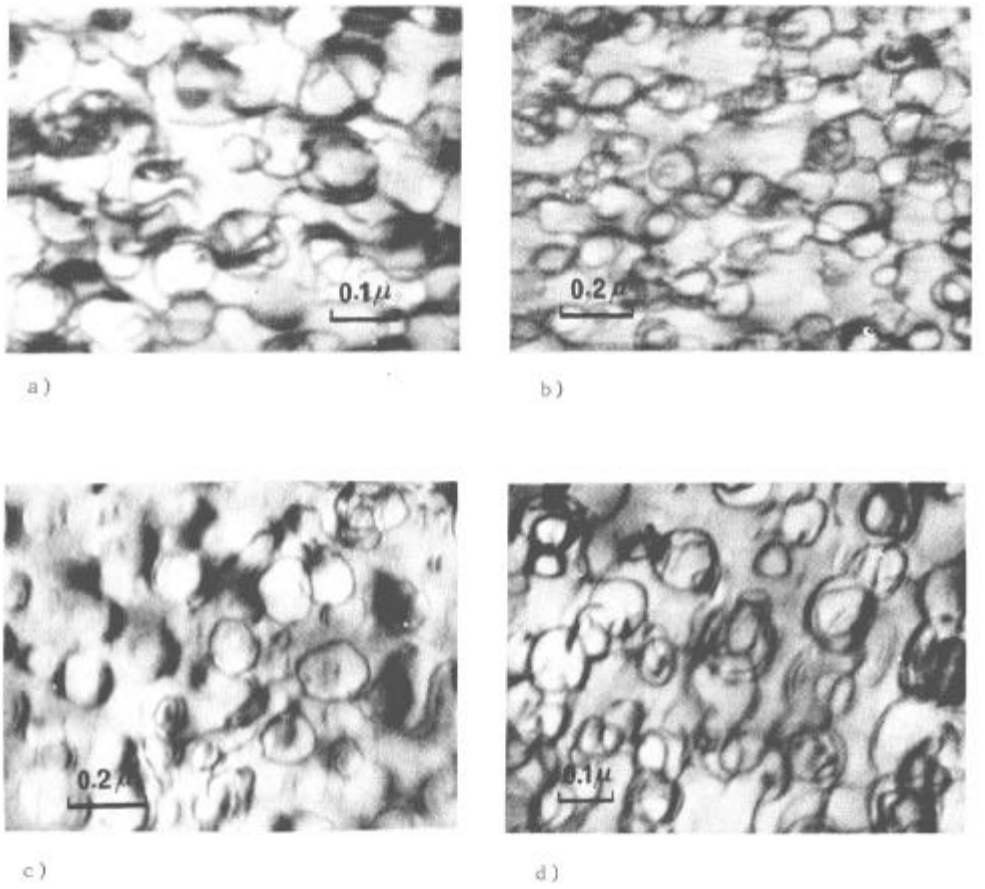

Fig. 1 - Transmission electron micrographs of specimens of the experimental alloy creep tested and stopped during the second stage: a) at 800°C under 314 MN/m^2; b) at 800°C under 274 MN/m^2; c) at 800°C under 206 MN/m^2; d) at 700°C under 490 MN/m^2. Bowing of dislocations between the γ' particles resulted in the pinched off dislocation loops.

0.2 mm. However the complex nature of the grain boundary morphology leads to different grain growths. In effect, as shown in Table I, the same solution treatment may produce a small difference in grain size, owing probably to differences in the extruded bars considered.

It might be expected that the resistance to dislocation motion would be dependent on the interaction of the dislocations with the gamma prime particles. However, variations in gamma prime size distribution were associated with marked changes in the dislocation structures. Ageing treatment at 900°C for 50^h produced spherical particles with an average size of approximately 1250 Å. When studied by transmission electron microscopy, contrast effects due to the presence of the gamma prime precipitates were observed, demonstrating their coherent nature.

Some samples of the experimental alloy creep tested at 800°C were stopped at the secondary creep and cooled under load to stabilize the structure at this stage. The distribution of dislocations was homogeneous and no evidence of localized deformation, pairs of dislocations or pile up of dislocations have been observed. At high stresses (314 and 274 MN/m^2 respectively) the dislocations bowed between gamma prime particles leaving pinched off dislocation loops (Figs. 1a, 1b). At lower stresses the creep tests examined (236 and 216 MN/m^2 respectively) showed that decreasing the stress decreases also the possibility of finding loops in the second creep stage.

Ageing treatments at 900°C for 15 and 90 hours respectively produce gamma prime particles approximately 950 and 1350 Å in diameter. Examinations of tested specimens exhibited dislocation structures similar to those previously represented. Many dislocations were observed bowing between particles and pinching off dislocation loops considering the samples creep tested at 800°C under 265 and 206 MN/m^2 (Fig. 1c) respectively.

Thin foils of the specimen creep tested at 700°C under 490 MN/m^2 exhibited also homogeneous distribution of dislocations with no evidence of localized deformation. In effect, the dislocations were found bounded around the particles to produce many dislocation loops (Fig. 1d). Thin foils from fractured specimens exhibited relatively high dislocation densities reflecting their high elongations.

Despite the low carbon content of the experimental alloy considered, in all the samples examined were present precipitates, probably primary carbide MC, distributed intragranular like needle/plate. Grain boundary precipitation also comprised discontinuous globular particles identified as $M_{23}C_6$ ([2]). For all heat treated materials, depletion of gamma prime adjacent to the grain boundaries occurred only in very limited areas.

In the primary creep deformation the strain data followed very well the Li equation derived for this stage. In fact the data calculated with this equation from the experimental curves are in a very good accordance with the experimental curves.

The results of the creep tests available from the alloy are reported in Table I.

The coefficients K_1 calculated from the experimental curves utilizing a computer programme of the Li equation, are presented

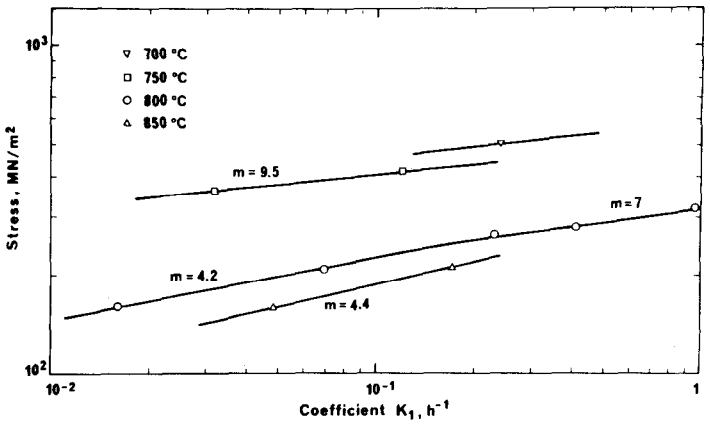

Fig. 2 - Effect of temperature on the coefficient K_1 from specimens of the experimental alloy heat treated 4^h 1150°C/AC + 50^h 900°C/AC.

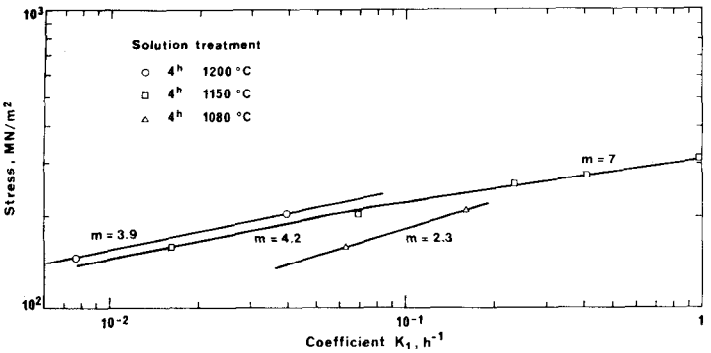

Fig. 3 - The dependence of the coefficient K_1 on stress at 800°C for different solution temperatures and an ageing treatment of 50^h at 900°C.

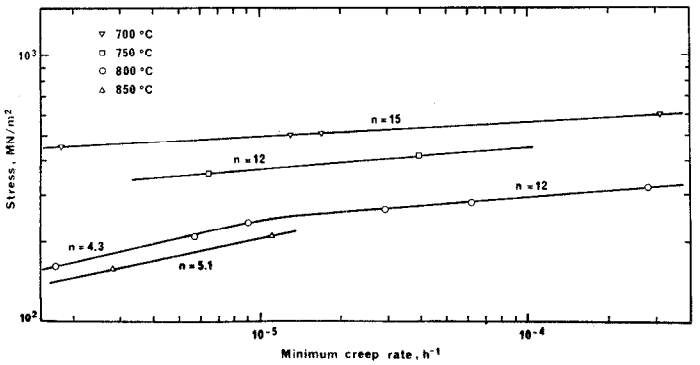

Fig. 4 - Effect of temperature on the minimum creep rate from specimens of the experimental alloy heat treated 4^h 1150°C/AC + 50^h 900°C/AC.

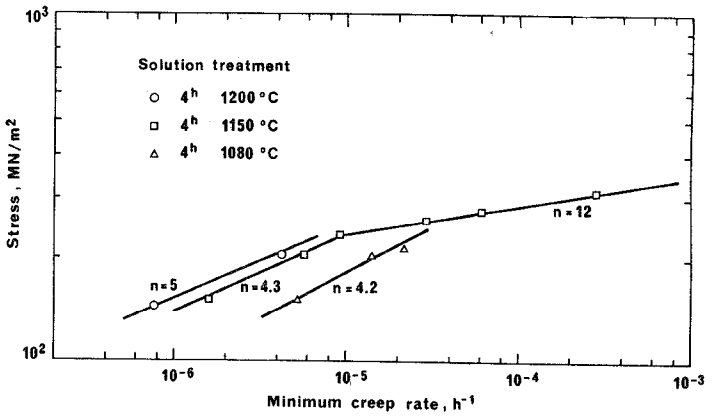

Fig. 5 - The dependence of the minimum creep rate on stress at 800°C for different solution temperatures and an ageing treatment of 50^h at 900°C.

in Fig. 2 as a function of stress and temperature. The coefficient K_1 depends on stress according to the relationship $K_1=B\sigma^m$, where B is a function of the temperature and the stress exponent m is about 4 (4.2 and 4.4 at 800 and 850°C respectively) for stresses below 240 MN/m^2 and about 8 (9.5 and 7 at 750 and 800°C respectively) at higher stresses. For specimens with a grain size of about 0.12 mm a lower stress exponent is observed (Fig. 3) and the effect of grain size at 800°C for the material with a gamma prime particle diameter of about 1250 Å is shown in Fig. 6 for two test stresses.

The dependence of the minimum creep rate $\dot{\varepsilon}_m$, calculated from the experimental curves in the secondary creep stage, is shown in Fig. 4 as a function of stress and temperature. The data agree very well with the relationship $\dot{\varepsilon}=A\sigma^n$, where A is a parameter depending on temperature and the stress exponent n changes from about 5 (4.3 and 5.1 at 800 and 850°C respectively) to higher values (15, 12 and 12 at 700, 750 and 800°C respectively) for stresses above 240 MN/m^2. The material becomes weaker when decreasing grain size and the effect on the minimum creep rate and stress exponent at 800°C is shown in Figs. 5 and 6. It is evident from the figures that this effect is decreasing with increasing grain size. The creep data are also presented as iso-creep strain curves (Fig. 7) for 0.1, 0.2 and 0.5% of creep deformation. The dependence on stress change in the region of 250 MN/m^2 reflects probably the change of the dislocation mechanisms operative during the deformation, observed directly from the microstructural examinations.

Discussion

Primary and secondary creep characteristics must be considered in the design of high temperature applications. The basic understanding of the creep in this early stage has been improved first by determining the time functions and second by relating these functions to the rate-controlling mechanisms ([4-8]). There are experimental indications that during the early stages of creep deformation, the total dislocation density increases with strain indicating generation or multiplication of dislocations. Based on these concepts, Li([9]) derived this relationship for primary creep deformation:

$$\varepsilon = \frac{\dot{\varepsilon}_m}{K_1} \ln \left\{ 1 + \frac{\dot{\varepsilon}_i - \dot{\varepsilon}_m}{\dot{\varepsilon}_m} \left[1 - \exp - \left(K_1 t \right) \right] \right\} + \dot{\varepsilon}_m t \qquad (1)$$

The applicability of this equation in the study of creep behaviour of nickel base alloys in the early stages of deformation, has been considered by the author for Waspaloy and highlighted from the results coming from the development of this research ([10]). Therefore we may state that the creep behaviour strongly depends on the rate coefficient K_1 and on the minimum creep rate $\dot{\varepsilon}_m$ and that both these parameters are expected to be dependent on gamma prime morphology, dislocation interactions with the precipitate particles and grain boundary structures. In effect the main problem arising from this study is to explain in quantitative manner this correlation.

To examine the effect of the grain size on the coefficient K_1 and on the minimum creep rate $\dot{\varepsilon}_m$, specimens of the alloy have been heat treated to produce a constant gamma prime particle diameter (≃ 1250 Å) and a range of grain sizes from about 0.1 to 0.4 mm and then tested at 800°C under two applied stresses (157 and 206 MN/m^2).

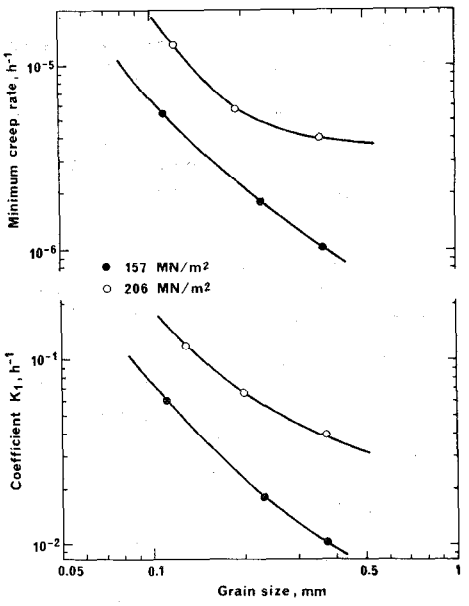

Fig. 6 - Effect of grain size on the minimum creep rate and on the coefficient K_1 at 800°C.

The results actually available show that these parameters have a similar behaviour corresponding to a decreasing effect when increasing the grain size diameters more than 0.25 mm. A possible explanation of this effect is that the decrease in grain size could become significant mechanisms such as diffusion creep, grain boundary sliding or grain boundary deformation, all with a lower stress exponent, with respect to the intragranular deformation process due to the dislocation motion mechanisms, that should be considered predominant when increasing the grain diameter above 0.25 mm. In effect, Figures 3 and 5 clearly show that the stress exponents of the coefficient K_1 and the minimum creep rate $\dot{\varepsilon}_m$ decrease when decreasing the grain size diameter from 0.35 mm to 0.12 mm.

The influence of the microstructure on the creep behaviour has been derived observing samples of the alloy heat treated to produce, while keeping constant the grain size, different gamma prime particle diameters and creep tested them at different stresses.

The microstructural examinations on samples, creep tested and stopped in the second stage, indicate that in all cases the dislocations did not shear precipitated particles but that their distribution was homogeneous. The dislocations by-passed the coherent gamma prime particles leaving off dislocation loops around these in the region of high stress exponents. Starting from 236 MN/m^2 and for lower stresses, the dislocation motion mechanism changes to-passing by climb.

Theoretically at each temperature there is a critical resolved shear stress (CRSS) above which the dislocations do not climb over the precipitated particles, greater than a critical size, but by-pass them by formation of loops. This concept was first considered by Orowan ([11]), and the following formulation of the CRSS was reported subsequently by Ashby ([12]):

$$\Delta\tau_o = AB\mu b \ (\ln d/4b) \ / \ 2\pi(\lambda-d) \qquad (2)$$

where μ is the matrix shear modulus, b the Burgers vector, λ the mean planar center to center particle separation, d the mean particle size and B a statistical factor (0.85) related to the occurrence of a distribution in interparticle spacing. A is a constant equal to 1 for edge dislocation and $(1-\nu)^{-1}$ for screw dislocation, where ν is Poisson's ratio.

In effect the stress required to permit dislocation bowing should be increased by the critical resolved shear stress of the solid solution without γ' precipitate. But considering this contribution very small, the CRSS $\Delta\tau_o$ values calculated from the equation (2) multiplied by the Taylor's factor could be compared directly to the applied stresses. The factor of 3.06 which was used for the present calculation may be considered to be an upper limit for this stress conversion.

Considering that the actual gamma prime particle diameter is about 1250 Å, the dislocation mechanism is expected to change at about 260 MN/m^2 at 850°C, 270 MN/m^2 at 800°C and 285 MN/m^2 at 700°C. With the approximations involved, the agreement between theoretical and experimental values is surprisingly good. It is interesting to observe that the same agreement was found by the author also for TD-Ni,Cr ([14]).

The temperature dependence can be described considering the minimum creep rate at a given particle diameter ($\simeq$ 1250 Å) with constant grain size ($\simeq$ 0.2 mm). At low stresses in the region of the low stress exponent ($n \simeq 5$) the activation energy for creep was measured by the temperature - increasing technique from 800 to 850°C and the value was about 45 Kcal/mol whereas at high stresses, in the region of high stress exponent ($n \simeq 12$), it was recorded at about 195 Kcal/mol.

The theory of Ansell and Weertman ([15]) predicts that, at constant particle size and spacing, a stress exponent of unity would be expected at low stresses, increasing to a value of a ~ 4 above the stress that allows the dislocations to bow between the particles. Furthermore the activation energy for creep should be equal to that for self-diffusion in the matrix ($E_D \sim 65$ Kcal/mol for Ni-Cr base alloys).

While the observed values of n and activation energy were not in agreement with the quantitative prediction of the theory, their model can account qualitatively for a number of the present results as it has been reported previously also for other two-phase alloys ([16]).

Moreover considering the activation volumes at 800°C for stresses below and above the critical stress at which occurs Orowan mechanism, values of 0.8 and 8.1 nm^3 have been measured respectively. These values are consistent with the dislocation motion mechanisms operative in the two stress regions. In fact the dislocation motion mechanisms controls the creep behaviour through the very sharp change of the stress exponent m and n, respectively for the coefficient K_1 and the minimum creep rate $\dot{\varepsilon}_m$ in the region in which it is expected to change the dislocation mechanism.

To examine the effect of gamma prime particle size on the creep rate coefficients K_1 and $\dot{\varepsilon}_m$, specimens of all the alloys considered in this project will be heat treated to produce a range of particle size and interparticle spacing λ. For the present alloy three particle sizes have been considered and the creep resistance decreases very sharply increasing the gamma prime par-

ticle size. However a better understanding of the effect of the microstructure on the creep rate coefficients K_1 and $\dot{\varepsilon}_m$ will be achieved when all the alloys, with different values of gamma prime volume fraction, will be considered.

The topic presented permitted correlations to be established for primary and second creep stage. Based on these relationships, some conclusions of practical importance can be drawn. In effect an important factor in high temperature design is the long time creep characteristics (0.1, 0.2% of deformation). It is usually impractical to conduct prolonged time tests to verify the applicability of a material for service. Consequently, the characteristics can be determined from shorter time tests (high temperature). Extrapolation of creep data can be accomplished using equation (1) in the primary stage and the remainder of creep deformation in the second stage considering $\varepsilon = \dot{\varepsilon}_m t$. This entailed evaluation of time for primary creep.

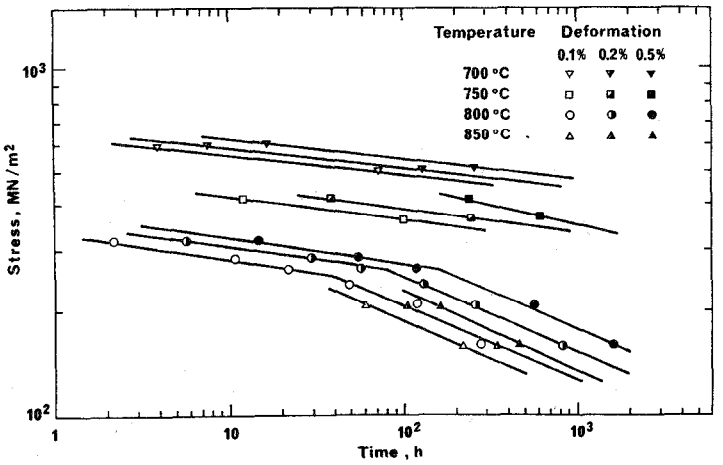

Fig. 7 - Iso-creep strain curves at different temperatures of the experimental alloy heat treated 4^h 1150°C + 50^h 900°C.

The primary creep rate decreases with time until it equals the minimum creep rate. Thus, $\dot{\varepsilon} = C\dot{\varepsilon}_m$ (C>1) during primary creep. Substituting in the equation (1), one obtains :

$$t = - (1/K_1) \ln (1-1/C) \qquad (3)$$

From a pratical point of view, primary creep can be considered complete when C is about 1.5. Based on this value, the times for primary creep were taken from the experimental curves. Thus iso-creep strain curves, like those presented in Fig. 7 from the actual data, can be extrapolated for stress (and time) of interest at temperatures of practical importance if relationship between K_1 and $\dot{\varepsilon}_m$ with stress, for a given microstructure, has been first established using relatively short time tests. In other words, the knowledge of the dislocation motion mechanisms operative during the creep deformation offers a basis for improving the accuracy of extrapolation of creep data in the range of the low deformations.

Acknowledgments

The author gratefully thanks Prof. P.M. Strocchi for his valuable discussion and encouragements, Mr. E. Bernocchi and Mr. E. Picco for conducting with skill and accuracy the creep tests and Mr. F. Gherardi for his assistance in electron microscopy.

This work has been carried out under the European Concerted Action on Materials for Gas Turbines (COST 50) with the collaboration of Istituto Ricerche Breda. Therefore thanks are due to Dr. W. Dumini for making some of the creep tests.

References

1. G.J. Lewis: Tech. Rep. N. 1333 H. Wiggin & Co. Ltd., 1971.

2. V. Lupinc and T.B. Gibbons: Prog. Rep. N. 1 COST 50, DMA 167, 1974.

3. O.H. Kriege and J.M. Baris: Trans. ASM, 1969, Vol. 62, p. 195.

4. G.A. Webster, A.P.D. Cox and J.E. Dorn: Met. Science Journal, 1969, Vol. 3, p. 221.

5. P.W. Davies, W.J. Evans, K.R. Williams and B. Wilshire: Scripta Met., 1969, Vol. 3, p. 671.

6. F. Garofalo, O. Richmond, W.F. Davies, F. Von Glenninger, Joint International Conference on Creep, London, 1963.

7. W.J. Evans and B. Wilshire: Trans. AIME, 1968, Vol. 242, p. 1303.

8. P.L. Treadgill, B. Wilshire: ISI Meeting on creep strength in steel and high temperature alloys, Sheffield, 1972.

9. J.C. Li: Acta Met., 1963, Vol. 11, p. 1269.

10. A. Ferrari: Seminar on structural stability, COST 50 - Prog. Rep. N. 2, Vienna, 1975.

11. E. Orowan: Symposium on internal stresses in metals and alloys, JISI, 1942, p. 451.

12. M.F. Ashby: "Physics of strength and plasticity", M.I.T. Press, 1969, p. 113.

13. H. Wiggin & Co. Ltd: private communication.

14. D.J. Wilson and A. Ferrari: Trans. ASME, J. of Eng. Mat. and Tech., 1974, Vol. 96, p. 109.

15. G.S. Ansell and J. Weertman: Trans. AIME, 1959, Vol. 215, p. 838.

16. P.L. Treadgill and B. Wilshire: Metal Science, 1974, Vol. 8, p. 117.